J. Fluid Mech. (1995), vol. 302, pp. 203–229

Third-harmonic wave diffraction by a vertical cylinder

By Š. MALENICA[1] AND B. MOLIN[2]

[1]Institut Français du Pétrole, BP 311, 92506 Rueil-Malmaison, France

[2]Ecole Supérieure d'Ingénieurs de Marseille, 13451 Marseille Cedex 20, France

(Received 13 January 1995 and in revised form 18 May 1995)

The diffraction of regular waves by a vertical circular cylinder in finite depth water is considered, within the frame of potential theory. The wave slope kA is assumed to be small so that successive boundary value problems at orders kA, k^2A^2, and k^3A^3 can be formulated. Here we focus on the third-order (k^3A^3) problem but restrict ourselves to the triple-frequency component of the diffraction potential. The method of resolution is based on eigenfunction expansions and on the integral equation technique with the classical Green function expressed in cylindrical coordinates. Third-order (triple-frequency) loads are calculated and compared with experimental measurements and approximate methods based on long-wave theories.

1. Introduction

In the recent past there has been much concern in the offshore industry about the 'ringing' problem. Ringing is a phenomenon that has recently been seen in some deep-water structures such as tension leg platforms (TLP's) and gravity base towers, when their natural periods fall in the 3–5 s range. Model tests and measurements at sea have revealed bursts of resonance in design sea-states, i.e. sea-states with peak periods typically 3 to 5 times the resonant periods. Such ratios suggest that strongly nonlinear phenomena occur in the loading process.

Wave loads on large offshore structures are usually tackled within the framework of potential theory. For a vertical circular cylinder, at high Reynolds numbers, this approach is justified as long as the wave amplitude does not exceed the radius.

For a fixed structure, nonlinearities in the boundary value problem are confined to the dynamic and kinematic boundary conditions at the free surface. (For the loading other nonlinearities intervene owing to the quadratic term in the Bernoulli equation and to the pressure integration around the waterline.) When the free surface boundary conditions are linearized, resolution of the resulting linearized, or first-order, diffraction problem yields loads occuring at the wave frequencies and proportional to the wave amplitude. For a vertical cylinder the problem was first solved by Havelock in 1940 for infinite water depth and extended by Mac Camy & Fuchs to finite depth (e.g. see Mei 1983).

Development of the tension leg platform concept aroused interest in the next order of approximation: the second-order diffraction problem, where loads at the sum (and difference) frequencies of the wave components are produced. These loads, known as 'springing' loads, affect the tethers in moderate sea-states and must be accounted for when calculating their fatigue life.

Second-order diffraction theory has now become a well-established topic. After pioneering papers by Lighthill (1979) and Molin (1979), diffraction loads on vertical cylinders were given by Molin & Marion (1986) and Eatock Taylor & Hung (1987). Numerical methods were subsequently proposed that yield localized second-order pressures (instead of the global loads), or even the second-order potential in the complete fluid domain (Kim & Yue 1989; Scolan & Molin 1989; Chau & Eatock Taylor 1992). Springing loads are now calculated in a standard way for such complex structures as TLP's at their resonant frequencies (Chen & Molin 1991; Newman & Lee 1992; Eatock Taylor & Chau 1992).

As already described, higher-order than second-order theories are required to predict ringing loads. Rather than trying to extend diffraction theory to higher orders, many researchers are following a different route, whereby the complete nonlinear problem is solved in the time domain. In two dimensions, so-called numerical wave tanks have proved valuable tools to study such problems as wave generation, propagation, and diffraction on obstacles (e.g. see Cointe 1990). So it appears to be just a matter of adding another dimension and increasing the size of the problem. So far only very limited results in three dimensions have been given (e.g. Romate 1989; Ferrant 1994).

Another approach is based on the observation that ringing occurs in long waves, typically at ka values around 0.15–0.30, k being the wavenumber and a the radius. In such a long-wave regime, first-order diffraction loads are reasonably well predicted by the so-called Morison equation when only the inertia term is retained. It has been conjectured that the Morison equation, or extensions of the Morison equation, could then be used to predict the nonlinear components of the loading as well. Such extensions (accounting for the quadratic term in the Bernoulli equation, and for spatial gradients in the incoming flow) have been proposed by Madsen (1986) and Rainey (1989), and used to predict ringing behaviour (Jefferys & Rainey 1994). More recently Faltinsen, Newman & Vinje (1995) have produced a low-ka low-kA theory (A being the wave amplitude), that gives the lowest-order approximations (in terms of ka) to the $O(k^2A^2)$ (second-order) and $O(k^3A^3)$ (third-order) loads. It should be noted that their approach differs from the one followed here in the sense that they assume the radius a and the wave amplitude A to be of the same order.

To establish the domain of validity of such approximations, 'exact' results are needed. Comparisons with experimental results may be considered. Unfortunately, for the time being, physical experiments do not appear to be a tool reliable enough to produce such elaborate information as third-order (triple-frequency) loads.

These considerations have motivated the present study, where we calculate exactly the third-order loads on a fixed vertical cylinder in finite depth. By 'exactly' we mean according to the classical Stokes perturbation scheme: the wave amplitude (or steepness) is of order ϵ, but the wavelength and radius are unrestricted (order 1). In the next section we develop the general equations of the problem, and formulate the boundary value problems (BVP) satisfied by the diffraction potential, at first, second, and third orders. Associated expressions for the loads are given. The following section is devoted to the resolution of these problems. It is based on eigenfunction expansions and use of the Green function in cylindrical coordinates. Thanks to the geometry the second-order diffraction potential can be obtained semi-analytically in a manner similar to the one proposed by Chau & Eatock Taylor (1992). The procedure is then extended to the calculation of the third-order (triple-frequency) loads contributed by the third-order diffraction potential. These computations involve intricate numerical integrations on the complete free surface. In the last section a comparison is made with available experimental results, which exhibit a large scatter and do not permit full validatation of our numerical results. They are then compared with those given by the long-wave theory of Faltinsen *et al.* (1995), and the overlap region is found to be reduced to very small values of the non-dimensional wavenumber ka.

2. General equations

2.1. *Boundary value problems*

Classical assumptions of perfect fluid and irrotational flow are made. We define a right-handed coordinate system (x, y, z), with $z = 0$ the undisturbed free surface, the axis z pointing upward and coinciding with the cylinder axis. The cylinder is standing on the sea bottom, assumed to be horizontal at $z = -H$. The cylindrical coordinate system (r, θ, z) will be used most often. The incoming wave system propagates along the x-axis.

The flow can be described by a velocity potential $\Phi(x, y, z, t)$ that obeys the following equations.

In the fluid:

$$\Delta\Phi = 0. \tag{2.1}$$

Combination of the dynamic and kinematic conditions at the free-surface results in:

$$\left\{\frac{\partial^2\Phi}{\partial t^2} + g\frac{\partial\Phi}{\partial z} + 2\nabla\Phi\cdot\nabla\frac{\partial\Phi}{\partial t} + \tfrac{1}{2}\nabla\Phi\cdot\nabla(\nabla\Phi\cdot\nabla\Phi) = 0\right\}_{z=\Xi} \tag{2.2}$$

where $\Xi(x, y, t)$ is the free surface elevation

$$\Xi = \left\{-\frac{1}{g}\left(\frac{\partial\Phi}{\partial t} + \tfrac{1}{2}\nabla\Phi\cdot\nabla\Phi\right)\right\}_{z=\Xi}. \tag{2.3}$$

On the cylinder wall and sea floor the no-flow condition is written:

$$\nabla\Phi\cdot\boldsymbol{n} = \boldsymbol{0}, \tag{2.4}$$

and finally an appropriate radiation condition must be satisfied at infinity. The convention used throughout this paper is that the normal vector $\boldsymbol{n}$ is pointing out of the fluid domain.

The main difficulty lies in the free surface conditions which are nonlinear and are written at an unknown position. To overcome this problem we proceed in the classical way suggested by Stokes. First we assume that the displacements of the free surface are small and we express quantities at the exact free surface by Taylor series developments based on the mean free surface position. We write

$$f(\Xi) = f(0) + \Xi\left.\frac{\partial f(z)}{\partial z}\right|_{z=0} + \frac{1}{2}\Xi^2\left.\frac{\partial^2 f(z)}{\partial z^2}\right|_{z=0} + O(\Xi^3). \tag{2.5}$$

This gives for the free surface elevation

$$\Xi = -\frac{1}{g}\left(\frac{\partial\Phi}{\partial t} + \tfrac{1}{2}\nabla\Phi\cdot\nabla\Phi - \frac{1}{g}\frac{\partial\Phi}{\partial t}\frac{\partial^2\Phi}{\partial t\partial z}\right) + O(\Phi^3) \tag{2.6}$$

and for the free surface condition

$$\frac{\partial^2 \Phi}{\partial^2 t} + g\frac{\partial \Phi}{\partial z} = -2\nabla\Phi \cdot \nabla\frac{\partial \Phi}{\partial t} - \tfrac{1}{2}\nabla\Phi \cdot \nabla(\nabla\Phi \cdot \nabla\Phi) + \frac{1}{g}\frac{\partial \Phi}{\partial t}\left(\frac{\partial^3 \Phi}{\partial t^2 \partial z} + g\frac{\partial^2 \Phi}{\partial z^2}\right)$$
$$+ \frac{2}{g}\frac{\partial \Phi}{\partial t}\left(\nabla\frac{\partial \Phi}{\partial z} \cdot \nabla\frac{\partial \Phi}{\partial t} + \nabla\Phi \cdot \nabla\frac{\partial^2 \Phi}{\partial t \partial z}\right)$$
$$- \frac{1}{g}\left(\frac{1}{g}\frac{\partial \Phi}{\partial t}\frac{\partial^2 \Phi}{\partial t \partial z} - \tfrac{1}{2}\nabla\Phi \cdot \nabla\Phi\right)\left(\frac{\partial^3 \Phi}{\partial t^2 \partial z} + g\frac{\partial^2 \Phi}{\partial z^2}\right)$$
$$- \frac{1}{2g^2}\left(\frac{\partial \Phi}{\partial t}\right)^2\left(\frac{\partial^4 \Phi}{\partial t^2 \partial z^2} + g\frac{\partial^3 \Phi}{\partial z^3}\right) + O(\Phi^4), \tag{2.7}$$

this equation being applied at the mean position of the free surface $z = 0$.

The next step is the introduction of the perturbation series with respect to wave steepness ($\varepsilon = k_0 A$ with k_0 the wavenumber, A the wave amplitude):

$$\Phi = \varepsilon\phi^{(1)} + \varepsilon^2\phi^{(2)} + \varepsilon^3\phi^{(3)} + O(\varepsilon^4). \tag{2.8}$$

Also we assume time periodicity at frequency ω for the flow at first order:

$$\varepsilon\phi^{(1)} = \mathrm{Re}\{\varphi^{(1)}\mathrm{e}^{-\mathrm{i}\omega t}\}, \tag{2.9}$$

from which we easily deduce the form of the higher-order potentials:

$$\varepsilon^2\phi^{(2)} = \bar{\varphi}^{(2)} + \mathrm{Re}\{\varphi^{(2)}\mathrm{e}^{-2\mathrm{i}\omega t}\}, \tag{2.10}$$

$$\varepsilon^3\phi^{(3)} = \mathrm{Re}\{\bar{\varphi}^{(3)}e^{-\mathrm{i}\omega t}\} + \mathrm{Re}\{\varphi^{(3)}\mathrm{e}^{-3\mathrm{i}\omega t}\}. \tag{2.11}$$

As stated in the introduction we are interested only in high-frequency phenomena. So the potentials $\bar{\varphi}^{(2)}$ and $\bar{\varphi}^{(3)}$ will be discarded. The same perturbation series is assumed for the free surface elevation Ξ:

$$\begin{aligned}\Xi &= \varepsilon\Xi^{(1)} + \varepsilon^2\Xi^{(2)} + \varepsilon^3\Xi^{(3)} + O(\varepsilon^4)\\ &= \mathrm{Re}\{\eta^{(1)}\mathrm{e}^{-\mathrm{i}\omega t}\} + \bar{\eta}^{(2)} + \mathrm{Re}\{\eta^{(2)}\mathrm{e}^{-2\mathrm{i}\omega t}\} + \mathrm{Re}\{\bar{\eta}^{(3)}\mathrm{e}^{-\mathrm{i}\omega t}\} + \mathrm{Re}\{\eta^{(3)}\mathrm{e}^{-3\mathrm{i}\omega t}\} + O(\varepsilon^4),\end{aligned} \tag{2.12}$$

After introduction of the perturbation series for the potential in the original free surface condition we obtain the following free surface conditions and free surface elevations at the corresponding orders:

$O(\varepsilon)$

$$-\nu\varphi^{(1)} + \frac{\partial \varphi^{(1)}}{\partial z} = 0, \tag{2.13}$$

$$\eta^{(1)} = \frac{\mathrm{i}\omega}{g}\varphi^{(1)}; \tag{2.14}$$

$O(\varepsilon^2)$

$$-4\nu\varphi^{(2)} + \frac{\partial \varphi^{(2)}}{\partial z} = \frac{\mathrm{i}\omega}{g}\left[\nabla\varphi^{(1)} \cdot \nabla\varphi^{(1)} - \tfrac{1}{2}\varphi^{(1)}\left(\frac{\partial^2 \varphi^{(1)}}{\partial z^2} - \nu\frac{\partial \varphi^{(1)}}{\partial z}\right)\right], \tag{2.15}$$

$$\eta^{(2)} = \frac{2\mathrm{i}\omega}{g}\varphi^{(2)} - \frac{1}{4g}\nabla\varphi^{(1)} \cdot \nabla\varphi^{(1)} - \frac{\nu^2}{2g}\varphi^{(1)}\varphi^{(1)}; \tag{2.16}$$

$O(\varepsilon^3)$

$$-9\nu\varphi^{(3)} + \frac{\partial\varphi^{(3)}}{\partial z} = \frac{3\mathrm{i}\omega}{g}\nabla\varphi^{(2)}\cdot\nabla\varphi^{(1)} - \frac{\mathrm{i}\omega}{2g}\left[\varphi^{(1)}\left(\frac{\partial^2\varphi^{(2)}}{\partial z^2} - 4\nu\frac{\partial\varphi^{(2)}}{\partial z}\right)\right.$$
$$\left. +2\varphi^{(2)}\left(\frac{\partial^2\varphi^{(1)}}{\partial z^2} - \nu\frac{\partial\varphi^{(1)}}{\partial z}\right)\right]$$
$$-\frac{1}{8g}\nabla\varphi^{(1)}\cdot\nabla(\nabla\varphi^{(1)}\cdot\nabla\varphi^{(1)}) - \frac{\nu}{g}\varphi^{(1)}\nabla\varphi^{(1)}\cdot\nabla\frac{\partial\varphi^{(1)}}{\partial z}$$
$$+\frac{1}{4g}\left(\nu\varphi^{(1)}\frac{\partial\varphi^{(1)}}{\partial z} + \tfrac{1}{2}\nabla\varphi^{(1)}\cdot\nabla\varphi^{(1)}\right)\left(\frac{\partial^2\varphi^{(1)}}{\partial z^2} - \nu\frac{\partial\varphi^{(1)}}{\partial z}\right) \quad (2.17)$$

where $\nu = \omega^2/g$ Also, all these potentials must satisfy the Laplace equation in the fluid domain, the no-flow condition on the fixed boundaries and adequate radiation conditions which will be discussed later.

2.2. *Wave loads*

They are calculated by integration of the pressure over the time-varying wetted surface of the cylinder:

$$\boldsymbol{F} = \iint_{S_B} p\boldsymbol{n}\mathrm{d}S \quad (2.18)$$

where the pressure is calculated from the Bernoulli equation:

$$p = -\varrho g z - \varrho\frac{\partial\Phi}{\partial t} - \tfrac{1}{2}\varrho(\nabla\Phi)^2. \quad (2.19)$$

In order to collect the terms at the different orders in ε the integral on the wetted surface is decomposed in two parts:

$$\iint_{S_B} = \iint_{S_{B0}} + \iint_{\Delta S} = \iint_{S_{B0}} + \int_{C_{B0}}\int_0^{\Xi} p\,\boldsymbol{n}\,\mathrm{d}z\,\mathrm{d}C, \quad (2.20)$$

S_{B0} being the mean wetted surface and C_{B0} the mean waterline.

The loads are decomposed as:

$$\boldsymbol{F} = \varepsilon\boldsymbol{F}^{(1)} + \varepsilon^2\boldsymbol{F}^{(2)} + \varepsilon^3\boldsymbol{F}^{(3)} + O(\varepsilon^4)$$
$$= \mathrm{Re}\{\mathscr{F}^{(1)}\mathrm{e}^{-\mathrm{i}\omega t}\} + \bar{\mathscr{F}}^{(2)} + \mathrm{Re}\{\mathscr{F}^{(2)}\mathrm{e}^{-2\mathrm{i}\omega t}\} + \mathrm{Re}\{\bar{\mathscr{F}}^{(3)}\mathrm{e}^{-\mathrm{i}\omega t}\} + \mathrm{Re}\{\mathscr{F}^{(3)}\mathrm{e}^{-3\mathrm{i}\omega t}\} + O(\varepsilon^4) \quad (2.21)$$

and the following expressions are obtained at the first three orders:

$O(\varepsilon)$

$$\mathscr{F}^{(1)} = \iint_{S_{B0}} i\omega\varrho\varphi^{(1)}\boldsymbol{n}\mathrm{d}S, \quad (2.22)$$

$O(\varepsilon^2)$

$$\mathscr{F}^{(2)} = \iint_{S_{B0}} (2\mathrm{i}\omega\varrho\varphi^{(2)} - \tfrac{1}{4}\varrho\nabla\varphi^{(1)}\cdot\nabla\varphi^{(1)})\boldsymbol{n}\mathrm{d}S + \tfrac{1}{4}\varrho g\int_{C_{B0}} \eta^{(1)}\eta^{(1)}\boldsymbol{n}\mathrm{d}C, \quad (2.23)$$

$O(\varepsilon^3)$

$$\mathscr{F}^{(3)} = \iint_{S_{B0}} \left(3\mathrm{i}\omega\varrho\varphi^{(3)} - \tfrac{1}{2}\varrho\nabla\varphi^{(1)}\cdot\nabla\varphi^{(2)} \right) \boldsymbol{n}\mathrm{d}S + \tfrac{1}{2}\varrho g \int_{C_{B0}} \eta^{(1)}(\eta^{(2)} - \tfrac{1}{4}\nu\eta^{(1)}\eta^{(1)}) \boldsymbol{n}\mathrm{d}C. \tag{2.24}$$

3. Calculation of the potentials

The boundary value problems for the potentials at the different orders have the same form and the resolution will be discussed in the general case. Consider the following boundary value problem for the potential φ:

in the fluid

$$\Delta\varphi = 0, \tag{3.1}$$

at the free surface $z = 0$

$$-\alpha\varphi + \frac{\partial\varphi}{\partial z} = Q(r,\theta), \tag{3.2}$$

at the fixed boundaries (cylinder surface and bottom)

$$\frac{\partial\varphi}{\partial n} = 0, \tag{3.3}$$

and a radiation condition for the diffracted part which will be discussed in each particular case.

The following decomposition of the potential is introduced:

$$\varphi = \varphi_I + \varphi_D = \varphi_I + \varphi_{DI} + \varphi_{DD} \tag{3.4}$$

where φ_I denotes the incident potential, and φ_{DI} and φ_{DD} represent diffraction components.

The incident components are easy to calculate in all three cases because these potentials do not satisfy the condition on the body or the radiation condition. At the free surface they must satisfy

$$-\alpha\varphi_I + \frac{\partial\varphi_I}{\partial z} = Q_I(r,\theta) \tag{3.5}$$

where $Q_I(r,\theta)$ denotes the right-hand sides of the free surface conditions (2.15), (2.17), in which only the terms coming from direct products of incident potentials are retained.

The first part φ_{DI} of the diffraction potential is chosen to satisfy the condition on the cylinder and an homogeneous condition on the free surface. It follows that it satisfies the usual Sommerfeld radiation condition.

The B.V.P. is

$$\left.\begin{aligned}
&\Delta\varphi_{DI} = 0, && -H \leqslant z \leqslant 0,\\
&-\alpha\varphi_{DI} + \frac{\partial\varphi_{DI}}{\partial z} = 0, && z = 0,\\
&\frac{\partial\varphi_{DI}}{\partial n} = -\frac{\partial\varphi_I}{\partial n}, && r = a,\\
&\frac{\partial\varphi_{DI}}{\partial z} = 0, && z = -H,\\
&\lim\left[(k_0 r)^{1/2}\left(\frac{\partial\varphi_{DI}}{\partial r} - \mathrm{i}k_0\varphi_{DI}\right)\right] = 0, && r \to \infty,
\end{aligned}\right\} \tag{3.6}$$

where k_0 is the solution of $\alpha = k_0 \tanh k_0 H$.

The second part φ_{DD} of the diffraction potential satisfies the homogeneous condition on the cylinder and a non-homogeneous one at the free surface:

$$\left.\begin{aligned}
&\Delta\varphi_{DD} = 0, && -H \leqslant z \leqslant 0,\\
&-\alpha\,\varphi_{DD} + \frac{\partial\varphi_{DD}}{\partial z} = Q_D(r,\theta), && z = 0,\\
&\frac{\partial\varphi_{DD}}{\partial n} = 0, && r = a,\\
&\frac{\partial\varphi_{DD}}{\partial z} = 0, && z = -H,
\end{aligned}\right\} \tag{3.7}$$

and a radiation condition for $r \to \infty$, that needs to be made precise. The forcing term on the free surface $Q_D(r,\theta)$ contains all remaining terms in $Q(r,\theta)$ after subtraction of the pure incident contributions: $Q_D(r,\theta) = Q(r,\theta) - Q_I(r,\theta)$.

Since we consider the case of a circular cylinder and because of the symmetry of the flow about the x-axis we develop all quantities as cosine Fourier series:

$$f(r,\theta,z) = \sum_{m=0}^{\infty} \epsilon_m f_m(r,z)\cos m\theta \tag{3.8}$$

where ϵ_m is equal to 1 for $m = 0$ and 2 for $m > 0$.

3.1. *Potential* φ_{DI}

As explained earlier this potential is a standard linear diffraction potential and can be found easily, by eigenfunction expansions, in the form

$$\varphi_{DI} = \sum_{m=0}^{\infty} \epsilon_m [f_0(z)\beta_{m0}H_m(k_0r) + \sum_{n=1}^{\infty} f_n(z)\beta_{mn}K_m(k_nr)]\cos m\theta \tag{3.9}$$

where H_m are Hankel functions of the first kind $H_m = J_m + \mathrm{i}Y_m$, and K_m are modified Bessel functions. The functions $f_n(z)$ are defined by

$$f_0(z) = \frac{\cosh k_0(z+H)}{\cosh k_0H}, \qquad f_n(z) = \frac{\cos k_n(z+H)}{\cos k_nH} \tag{3.10}$$

with $\alpha = k_0 \tanh k_0H = -k_n \tan k_nH$.

If we express the incident potential as

$$\varphi_I = f_I(z)\sum_{m=0}^{\infty} \epsilon_m \varphi_{Im}(r)\cos m\theta \tag{3.11}$$

we can enforce the condition on the cylinder and obtain for the coefficients β_{mn} the following expressions:

$$\beta_{m0} = -\frac{2C_0}{k_0H_m'(k_0a)}\frac{\partial\varphi_{Im}}{\partial r}(a)\int_{-H}^{0} f_0(z)f_I(z)\mathrm{d}z, \tag{3.12}$$

$$\beta_{mn} = -\frac{2C_n}{k_nK_m'(k_na)}\frac{\partial\varphi_{Im}}{\partial r}(a)\int_{-H}^{0} f_n(z)f_I(z)\mathrm{d}z, \tag{3.13}$$

where C_0 and C_n are defined by

$$C_0 = \left[2\int_{-H}^{0} f_0^2(z)\mathrm{d}z\right]^{-1}, \quad C_n = \left[2\int_{-H}^{0} f_n^2(z)\mathrm{d}z\right]^{-1} \tag{3.14}$$

3.2. *Potential* φ_{DD}

This part of the potential is the most difficult to calculate because of the non-homogeneous condition on the free surface. The method which will be used is based on the use of the Green function expressed as a series of eigenfunctions.

Consider a Green function which satisfies the following set of equations:

$$\left.\begin{aligned}
&\Delta_\xi G(\boldsymbol{x},\boldsymbol{\xi}) = \delta(\boldsymbol{x}), && -H \leqslant \zeta \leqslant 0,\\
&-\alpha G + \frac{\partial G}{\partial \zeta} = 0, && \zeta = 0,\\
&\frac{\partial G}{\partial \zeta} = 0, && \zeta = -H,\\
&\lim\left[(k_0\rho)^{1/2}\left(\frac{\partial G}{\partial \rho} - ik_0 G\right)\right] = 0, && \rho \to \infty,
\end{aligned}\right\} \tag{3.15}$$

where $\boldsymbol{x}$ and $\boldsymbol{\xi}$ represent respectively the source point (r,θ,z) and the field point (ρ,ϑ,ζ). $\boldsymbol{\delta}$ is the Dirac delta function and Δ_ξ represents the Laplace operator with respect to the $\boldsymbol{\xi}$ variable.

The solution for $G(\boldsymbol{x},\boldsymbol{\xi})$ is well known (e.g. see Mei 1983) and can be written in the following form:

$$G(\boldsymbol{x},\boldsymbol{\xi}) = \sum_{m=0}^{\infty} \epsilon_m G_m(r,z;\rho,\zeta)\cos m(\theta-\vartheta), \tag{3.16}$$

with

$$\begin{aligned}
G_m(r,z;\rho,\zeta) = &-\frac{\mathrm{i}}{2}C_0\begin{pmatrix} H_m(k_0r)J_m(k_0\rho) \\ J_m(k_0r)H_m(k_0\rho)\end{pmatrix} f_0(z)f_0(\zeta)\\
&-\frac{1}{\pi}\sum_{n=1}^{\infty} C_n\begin{pmatrix} K_m(k_nr)I_m(k_n\rho) \\ I_m(k_nr)K_m(k_n\rho)\end{pmatrix} f_n(z)f_n(\zeta) \qquad \begin{pmatrix} r>\rho \\ r<\rho\end{pmatrix}.
\end{aligned} \tag{3.17}$$

We now write the classical integral equation

$$\begin{aligned}
\begin{pmatrix}\varphi_{DD}(\boldsymbol{x}) \\ 0\end{pmatrix} + \iint_{S_{B0}} \varphi_{DD}(\boldsymbol{\xi})\frac{\partial G(\boldsymbol{x},\boldsymbol{\xi})}{\partial \rho}\mathrm{d}S = &-\iint_{S_F} G(\boldsymbol{x},\boldsymbol{\xi})Q_D(\rho,\vartheta)\mathrm{d}S\\
&+\iint_{S_\infty}\left[G(\boldsymbol{x},\boldsymbol{\xi})\frac{\partial \varphi_{DD}(\boldsymbol{\xi})}{\partial \rho} - \varphi_{DD}(\boldsymbol{\xi})\frac{\partial G(\boldsymbol{x},\boldsymbol{\xi})}{\partial \rho}\right]\mathrm{d}S \qquad \begin{pmatrix} r>a \\ r<a\end{pmatrix}.
\end{aligned} \tag{3.18}$$

It can be shown (see Appendix A), although not quite rigorously, that the integral over the control surface at infinity S_∞ disappears at all three orders and this disappearence represents, in some way, the radiation condition for this part of the potential.

The next step is to develop the solution for φ_{DD} on the cylinder, as a series of eigenfunctions. For each Fourier mode we write

$$\varphi_{DDm}(a,z) = f_0(z)A_{m0} + \sum_{n=1}^{\infty} f_n(z)A_{mn}. \tag{3.19}$$

If we now write the integral equation for a point inside the cylinder, $r = a - \delta(a \geqslant \delta > 0)$ we can deduce the values of the A_{mn} coefficients by using the orthogonal properties of the eigenfunctions:

$$A_{m0} = -\frac{2C_0 \int_a^\infty H_m(k_0\rho)Q_{Dm}(\rho)\rho\mathrm{d}\rho}{k_0 a H_m'(k_0 a)}, \tag{3.20}$$

$$A_{mn} = -\frac{2C_n \int_a^\infty K_m(k_n\rho)Q_{Dm}(\rho)\rho\mathrm{d}\rho}{k_n a K_m'(k_n a)}. \tag{3.21}$$

By substituting these expressions into the integral equation we obtain the expression for the potential at any point in the fluid:

$$\begin{aligned}\varphi_{DDm}(r,z) = {} & \pi\mathrm{i}C_0 f_0(z)H_m(k_0r)\int_a^r [J_m(k_0\rho) - Z_{m0}H_m(k_0\rho)]Q_{Dm}(\rho)\rho\mathrm{d}\rho \\ & + 2\sum_{n=1}^{\infty} C_n f_n(z)K_m(k_nr)\int_a^r [I_m(k_n\rho) - Z_{mn}K_m(k_n\rho)]Q_{Dm}(\rho)\rho\mathrm{d}\rho \\ & + \pi\mathrm{i}C_0 f_0(z)[J_m(k_0r) - Z_{m0}H_m(k_0r)]\int_r^\infty H_m(k_0\rho)Q_{Dm}(\rho)\rho\mathrm{d}\rho \\ & + 2\sum_{n=1}^{\infty} C_n f_n(z)[I_m(k_nr) - Z_{mn}K_m(k_nr)]\int_r^\infty K_m(k_n\rho)Q_{Dm}(\rho)\rho\mathrm{d}\rho \end{aligned} \tag{3.22}$$

with

$$Z_{m0} = \frac{J_m'(k_0a)}{H_m'(k_0a)}, \qquad Z_{mn} = \frac{I_m'(k_na)}{K_m'(k_na)}. \tag{3.23}$$

This is the same expression as obtained by Chau & Eatock Taylor (1992) by using a modified Green function that satisfies the homogeneous condition on the cylinder. Although the solution is expressed as a series of eigenfunctions which individually satisfy the homogeneous free surface condition, it can be shown that the sum of the series satisfies the non-homogeneous condition when $z \to 0^-$ (Chau & Eatock Taylor 1992).

In order to calculate the forcing term $Q_D^{(3)}$ in the free surface condition for the third-order potential $\varphi^{(3)}$ we need to know the second-order potential $\varphi^{(2)}$ at the free surface, and some of its derivatives. So the logarithmic singularity that occurs in expression (3.22) for $\varphi_{DDm}^{(2)}$ must be treated carefully when evaluating these quantities (Fenton 1978; Chau & Eatock Taylor 1992). For details we refer to Malenica (1994).

4. First-order potential

The solution for this potential is well known and we just recall it here:

$$\varphi_I^{(1)} = -\frac{\mathrm{i}gA}{\omega} f_0^{(1)}(z)\mathrm{e}^{\mathrm{i}k_0x} = -\frac{\mathrm{i}gA}{\omega} f_0^{(1)}(z)\sum_{m=0}^{\infty}\epsilon_m \mathrm{i}^m J_m(k_0r)\cos m\theta, \tag{4.1}$$

$$\varphi_{DI}^{(1)} = \frac{\mathrm{i}gA}{\omega} f_0^{(1)}(z)\sum_{m=0}^{\infty}\epsilon_m \mathrm{i}^m Z_{m0}^{(1)} H_m(k_0r)\cos m\theta, \tag{4.2}$$

$$\varphi_{DD}^{(1)} = 0, \tag{4.3}$$

with $\nu = \omega^2/g = k_0 \tanh k_0 H$ and $Z_{m0}^{(1)} = J_m'(k_0a)/H_m'(k_0a)$.

5. Second-order potential

In this case the coefficient α is 4ν and the forcing term on the free surface is

$$Q^{(2)}(r,\theta) = \frac{\mathrm{i}\omega}{g}\left[\nabla\varphi^{(1)}\cdot\nabla\varphi^{(1)} - \tfrac{1}{2}\varphi^{(1)}\left(\frac{\partial^2\varphi^{(1)}}{\partial z^2} - \nu\frac{\partial\varphi^{(1)}}{\partial z}\right)\right] \tag{5.1}$$

which in the case of a fixed cylinder can be written as

$$Q^{(2)}(r,\theta) = \frac{\mathrm{i}\omega}{2g}(3\nu^2 - k_0^2)\varphi^{(1)^2} + \frac{\mathrm{i}\omega}{g}\nabla_0\varphi^{(1)}\cdot\nabla_0\varphi^{(1)} \tag{5.2}$$

with ∇_0 denoting the horizontal gradient

$$\nabla_0 = \left(\frac{\partial}{\partial r}, \frac{1}{r}\frac{\partial}{\partial\theta}, 0\right).$$

5.1. *Incident second-order potential $\varphi_I^{(2)}$*

The forcing term $Q_I^{(2)}(r,\theta)$ is given by

$$Q_I^{(2)}(r,\theta) = \frac{\mathrm{i}\omega}{2g}(3\nu^2 - k_0^2)\varphi_I^{(1)^2} + \frac{\mathrm{i}\omega}{g}\nabla_0\varphi_I^{(1)}\cdot\nabla_0\varphi_I^{(1)} = \frac{3\mathrm{i}\omega A^2}{2}\frac{\nu}{\sinh^2 k_0H}\mathrm{e}^{2\mathrm{i}k_0r\cos\theta}. \tag{5.3}$$

The potential which satisfies the free surface condition with this forcing term, the Laplace equation in the fluid and the no-flow condition on the bottom is also well known:

$$\begin{aligned}\varphi_I^{(2)} &= -\frac{3\mathrm{i}\omega A^2}{8}\frac{\cosh 2k_0(z+H)}{\sinh^4 k_0H}\mathrm{e}^{2\mathrm{i}k_0r\cos\theta} \\ &= -\frac{3\mathrm{i}\omega A^2}{8}\frac{\cosh 2k_0(z+H)}{\sinh^4 k_0H}\sum_{m=0}^{\infty}\epsilon_m\mathrm{i}^m J_m(2k_0r)\cos m\theta.\end{aligned} \tag{5.4}$$

5.2. *Second-order diffraction potential $\varphi_{DI}^{(2)}$*

The general solution is given in §3.1 and it can be applied in a straightforward manner. We define the wavenumbers κ_0, κ_n as

$$4\nu = \kappa_0\tanh\kappa_0H = -\kappa_n\tan\kappa_nH. \tag{5.5}$$

One needs only to apply equations (3.12) and (3.13) where

$$f_I^{(2)}(z) = -\frac{\cosh 2k_0(z+H)}{4\nu\sinh^2 k_0H}, \qquad \varphi_{Im}^{(2)}(r) = \frac{3\mathrm{i}\omega A^2}{2}\frac{\nu}{\sinh^2 k_0H}\mathrm{i}^m J_m(2k_0r) \tag{5.6}$$

and the z integrals are given by

$$\int_{-H}^{0} f_0^{(2)}(z)f_I^{(2)}(z)\mathrm{d}z = \frac{1}{4k_0^2 - \kappa_0^2}, \qquad \int_{-H}^{0} f_n^{(2)}(z)f_I^{(2)}(z)\mathrm{d}z = \frac{1}{4k_0^2 + \kappa_n^2}. \tag{5.7}$$

5.3. *Second-order diffraction potential $\varphi_{DD}^{(2)}$*

The general solution for this part of the potential is given by (3.22). In the second-order case the forcing term $Q_D^{(2)}(r,\theta)$ is given by

$$Q_D^{(2)}(r,\theta) = \frac{\mathrm{i}\omega}{2g}(3\nu^2 - k_0^2)(\varphi_D^{(1)^2} + 2\varphi_I^{(1)}\varphi_D^{(1)}) + \frac{\mathrm{i}\omega}{g}(\nabla_0\varphi_D^{(1)}\cdot\nabla_0\varphi_D^{(1)} + 2\nabla_0\varphi_I^{(1)}\cdot\nabla_0\varphi_D^{(1)}). \tag{5.8}$$

Knowing explicitely the first-order potential we can easily calculate the Fourier modes $Q_{Dm}(r)$, by using the following identities:

$$\left.\begin{aligned}\sum_{m=0}^{\infty}\epsilon_m\alpha_m\cos m\theta\sum_{n=0}^{\infty}\epsilon_n\beta_n\cos n\theta &= \sum_{m=0}^{\infty}\epsilon_m\left[\sum_{n=1}^{\infty}(\alpha_n\beta_{m+n}+\alpha_{m+n}\beta_n)\right.\\ &\qquad\left.+\sum_{n=0}^{m}\alpha_{m-n}\beta_n\right]\cos m\theta,\\ \sum_{m=0}^{\infty}\epsilon_m\alpha_m\sin m\theta\sum_{n=0}^{\infty}\epsilon_n\beta_n\sin n\theta &= \sum_{m=0}^{\infty}\epsilon_m\left[\sum_{n=1}^{\infty}(\alpha_n\beta_{m+n}+\alpha_{m+n}\beta_n)\right.\\ &\qquad\left.-\sum_{n=0}^{m}\alpha_{m-n}\beta_n\right]\cos m\theta.\end{aligned}\right\}\tag{5.9}$$

Besides the problem of the singularity in the calculation of the potential $\varphi_{DD}^{(2)}$ on the free surface, which was briefly discussed in §3.2, there is another important problem in the application of equation (3.22), namely the treatment of the infinite oscillatory integral:

$$\int_r^{\infty} H_m(\kappa_0\rho)Q_{Dm}^{(2)}(\rho)\rho\mathrm{d}\rho.\tag{5.10}$$

To simplify this task we proceed in a similar way to that used by Kim & Yue (1989) or Chau & Eatock Taylor (1992). First of all we make use of the following identity to eliminate the radial derivative of the first-order potential in the expression for $Q_{Dm}^{(2)}$:

$$\begin{aligned}\iint_{S_F}\chi\nabla_0\varphi\nabla_0\psi\mathrm{d}S &= \frac{1}{2}\iint_{S_F}\left\{\varphi\psi\nabla_0^2\chi-\chi\left(\varphi\nabla_0^2\psi+\psi\nabla_0^2\varphi\right)\right\}\mathrm{d}S\\ &\quad-\frac{1}{2}\int_{C_r\cup C_\infty}\left\{\psi\varphi\frac{\partial\chi}{\partial n}-\chi\left(\varphi\frac{\partial\psi}{\partial n}+\psi\frac{\partial\varphi}{\partial n}\right)\right\}\mathrm{d}C.\end{aligned}\tag{5.11}$$

By setting $\chi = H_m(\kappa_0\rho)\cos m\vartheta$, $\varphi=\varphi_D^{(1)}$, $\psi=\varphi_D^{(1)}$ and then $\psi=\varphi_I^{(1)}$, we obtain

$$\begin{aligned}\int_r^{\infty} H_m(\kappa_0\rho)Q_{Dm}^{(2)}(\rho)\rho\mathrm{d}\rho &= \frac{\mathrm{i}\omega}{2g}(3\nu^2+k_0^2-\kappa_0^2)\int_r^{\infty}H_m(\kappa_0\rho)[\varphi_D^{(1)}\varphi_D^{(1)}+2\varphi_I^{(1)}\varphi_D^{(1)}]_m\rho\mathrm{d}\rho\\ &\quad+\frac{\mathrm{i}\omega}{2g}\left\{\frac{\partial H_m(\kappa_0\rho)}{\partial\rho}[\varphi_D^{(1)}\varphi_D^{(1)}+2\varphi_I^{(1)}\varphi_D^{(1)}]_m\rho\right.\\ &\quad\left.-2H_m(\kappa_0\rho)\left[\varphi_D^{(1)}\frac{\partial\varphi_D^{(1)}}{\partial\rho}+\varphi_I^{(1)}\frac{\partial\varphi_D^{(1)}}{\partial\rho}+\varphi_D^{(1)}\frac{\partial\varphi_I^{(1)}}{\partial\rho}\right]_m\rho\right\}_{\rho=r}.\end{aligned}\tag{5.12}$$

This simplifies the infinite oscillatory integrals which now involve only triple products of Hankel functions and can be calculated in the semi-analytical way proposed by the authors mentioned above. The numerical method which is used for the numerical part of the integration is the simple trapezoidal rule combined with Romberg quadrature. In fact we do not need more-sophisticated methods because we must calculate the second-order potential at points very close to the free surface anyway, in order to calculate its radial derivative numerically, by finite differentiation. So the infinite oscillatory integral (5.10) is calculated only once for $r = a$ and then we move from left to right by Δr and successive integrals are obtained by simple subtraction of the trapezoidal surface from r to $r+\Delta r$. Owing to the special treatment of the singularity at the free surface this procedure is not possible for the parts associated with the modified Bessel functions K_m, but these contributions being localized can be calculated for each point separately, with a sufficient accuracy and without very much computational effort.

6. Third-order potential

For the third-order problem the coefficient α is 9ν and the forcing term on the free surface is

$$\begin{aligned} Q^{(3)}(r,\theta) = {} & \frac{3\mathrm{i}\omega}{g}\nabla\varphi^{(2)}\cdot\nabla\varphi^{(1)} - \frac{\mathrm{i}\omega}{2g}\left[\varphi^{(1)}\left(\frac{\partial^2\varphi^{(2)}}{\partial z^2} - 4\nu\frac{\partial\varphi^{(2)}}{\partial z}\right)\right. \\ & \left. + 2\varphi^{(2)}\left(\frac{\partial^2\varphi^{(1)}}{\partial z^2} - \nu\frac{\partial\varphi^{(1)}}{\partial z}\right)\right] \\ & - \frac{1}{8g}\nabla\varphi^{(1)}\cdot\nabla(\nabla\varphi^{(1)}\cdot\nabla\varphi^{(1)}) - \frac{\nu}{g}\varphi^{(1)}\nabla\varphi^{(1)}\cdot\nabla\frac{\partial\varphi^{(1)}}{\partial z} \\ & + \frac{1}{4g}\left(\nu\varphi^{(1)}\frac{\partial\varphi^{(1)}}{\partial z} + \tfrac{1}{2}\nabla\varphi^{(1)}\cdot\nabla\varphi^{(1)}\right)\left(\frac{\partial^2\varphi^{(1)}}{\partial z^2} - \nu\frac{\partial\varphi^{(1)}}{\partial z}\right). \end{aligned} \quad (6.1)$$

$Q^{(3)}$ has two components: the first one, $Q_1^{(3)}(r,\theta)$, involves triple products of first-order quantities, whereas the second one, $Q_2^{(3)}(r,\theta)$, involves products of first-order and second-order quantities. As in the second-order case we can simplify their expressions, taking advantage of the geometry and of the fact that the cylinder is fixed:

$$\begin{aligned} Q_1^{(3)}(r,\theta) = {} & -\frac{1}{8g}[\nabla_0\varphi^{(1)}\cdot\nabla_0(\nabla_0\varphi^{(1)}\cdot\nabla_0\varphi^{(1)}) + (13\nu^2 - k_0^2)\varphi^{(1)}\nabla_0\varphi^{(1)}\cdot\nabla_0\varphi^{(1)} \\ & + \nu^2(7k_0^2 + 3\nu^2)\varphi^{(1)^3}], \end{aligned} \quad (6.2)$$

$$Q_2^{(3)}(r,\theta) = \frac{\mathrm{i}\omega}{g}\left\{3\nabla_0\varphi^{(1)}\cdot\nabla_0\varphi^{(2)} + \varphi^{(1)}\left[(21\nu^2 - k_0^2)\varphi^{(2)} + 5\nu Q^{(2)} - \frac{1}{2}\frac{\partial^2\varphi^{(2)}}{\partial z^2}\right]\right\}. \quad (6.3)$$

6.1. *Potential* $\varphi_I^{(3)}$

By introducing (4.1) and (5.4) in the above expressions we obtain for $Q_I^{(3)}(r,\theta)$

$$Q_I^{(3)}(r,\theta) = \frac{3\mathrm{i}\omega k_0^2 A^3}{8\sinh^4 k_0 H}(11 - 2\cosh 2k_0 H)\mathrm{e}^{3\mathrm{i}k_0 r\cos\theta} \quad (6.4)$$

and we deduce the third-order incident potential

$$\begin{aligned} \varphi_I^{(3)} & = -\frac{\mathrm{i}\omega k_0 A^3}{64}(11 - 2\cosh 2k_0 H)\frac{\cosh 3k_0(z+H)}{\sinh^7 k_0 H}\mathrm{e}^{3\mathrm{i}k_0 r\cos\theta} \\ & = -\frac{\mathrm{i}\omega k_0 A^3}{64}(11 - 2\cosh 2k_0 H)\frac{\cosh 3k_0(z+H)}{\sinh^7 k_0 H}\sum_{m=0}^{\infty}\epsilon_m \mathrm{i}^m J_m(3k_0 r)\cos m\theta. \end{aligned} \quad (6.5)$$

We observe that both the second-order and third-order incident potentials are zero in the case of infinite water depth (note again that we deal here only with the 3ω component of the third-order potential).

6.2. *Potential* $\varphi_{DI}^{(3)}$

The procedure is exactly the same as at second-order, with the wavenumbers μ_0, μ_n defined by

$$9\nu = \mu_0 \tanh \mu_0 H = -\mu_n \tan \mu_n H. \tag{6.6}$$

We now have

$$f_I^{(3)}(z) = -\frac{\cosh 3k_0(z+H)}{24k_0 \sinh^3 k_0 H}, \tag{6.7}$$

$$\varphi_{Im}^{(3)} = \frac{3\mathrm{i}\omega k_0^2 A^3}{8\sinh^4 k_0 H}(11 - 2\cosh 2k_0 H)\mathrm{i}^m J_m(3k_0 r). \tag{6.8}$$

The z integrals are

$$\int_{-H}^{0} f_0^{(3)}(z) f_I^{(3)}(z)\mathrm{d}z = \frac{1}{9k_0^2 - \mu_0^2}, \qquad \int_{-H}^{0} f_n^{(3)}(z) f_I^{(3)}(z)\mathrm{d}z = \frac{1}{9k_0^2 + \mu_n^2}. \tag{6.9}$$

6.3. *Potential* $\varphi_{DD}^{(3)}$

We shall only consider the contribution of the potential $\varphi_{DD}^{(3)}$ to the third-order force. From equation (2.24) this contribution is

$$F_{3DD}^{(3)} = -6\mathrm{i}\omega\varrho a\pi \int_{-H}^{0} \varphi_{DD1}^{(3)}\mathrm{d}z. \tag{6.10}$$

We can write

$$\int_{-H}^{0} \varphi_{DD1}^{(3)}\mathrm{d}z = -\int_{a}^{\infty} \left[\frac{18\nu C_0^{(3)}}{\mu_0^3 a H_1'(\mu_0 a)} H_1(\mu_0\rho) + \sum_{n=1}^{\infty} \frac{-18\nu C_n^{(3)}}{\mu_n^3 a K_1'(\mu_n a)} K_1(\mu_n\rho)\right] Q_{D1}^{(3)}(\rho)\mathrm{d}\rho. \tag{6.11}$$

As in the second-order case the main difficulty is associated with the calculation of the integrals over the free surface. The two contributions to $Q_D^{(3)}$, (6.2) and (6.3), will be treated separately. With the first one, calculations can be performed easily because the first-order potential is known explicitly and use of (5.9) for the products of two series gives the values of $Q_{1D}^{(3)}(r,\theta)$ without much computational effort. So we write simply

$$Q_{1D}^{(3)}(r,\theta) = Q_1^{(3)}(r,\theta) - Q_{1I}^{(3)}(r,\theta). \tag{6.12}$$

The second part $Q_{2D}^{(3)}(r,\theta)$ can be developed as follows:

$$\begin{aligned} Q_{2D}^{(3)}(r,\theta) = \frac{\mathrm{i}\omega}{g}\Big\{ & 3(\nabla_0\varphi^{(1)}\nabla_0\varphi_D^{(2)} + \nabla_0\varphi_D^{(1)}\nabla_0\varphi_I^{(2)}) \\ & + \varphi^{(1)}\left[(21\nu^2 - k_0^2)\varphi_D^{(2)} + 5\nu Q_D^{(2)} - \frac{1}{2}\frac{\partial^2\varphi_D^{(2)}}{\partial z^2}\right] \\ & + \varphi_D^{(1)}[(21\nu^2 - 3k_0^2)\varphi_I^{(2)} + 5\nu Q_I^{(2)}]\Big\}. \end{aligned} \tag{6.13}$$

The difficult terms are those which contain the potential $\varphi_D^{(2)}$. This potential, its radial derivative, and its double z derivative, all appear. By using the identity (5.11) we can avoid the calculation of either the double z derivative or the radial derivative. Here we have prefered to eliminate the double z derivative which is more complicated to calculate. To do this we use expression (5.11) in the form

$$\iint_{S_F} \chi\varphi^{(1)}\frac{\partial^2\varphi_D^{(2)}}{\partial z^2}\mathrm{d}S = 2\iint_{S_F}\chi\nabla_0\varphi^{(1)}\cdot\nabla_0\varphi_D^{(2)}\mathrm{d}S - \iint_{S_F}(\nabla_0^2\chi + k_0^2\chi)\varphi^{(1)}\varphi_D^{(2)}\mathrm{d}S$$
$$-\int_{C_a}\left[\varphi^{(1)}\varphi_D^{(2)}\frac{\partial\chi}{\partial\rho} - \chi\left(\varphi^{(1)}\frac{\varphi_D^{(2)}}{\partial\rho} + \frac{\partial\varphi^{(1)}}{\partial\rho}\varphi_D^{(2)}\right)\right]\mathrm{d}C \quad (6.14)$$

where the integral over C_∞ is omitted because it disappears in the same way as the integrals $I_\infty^{(3)}$ (see Appendix A).

This leads to the following expression:

$$\iint_{S_F}\chi Q_{2D}^{(3)}\mathrm{d}S = \iint_{S_F}\chi\tilde{Q}_{2D}^{(3)}\mathrm{d}S + \frac{\mathrm{i}\omega}{2g}\iint_{S_F}\nabla_0^2\chi\varphi^{(1)}\varphi_D^{(2)}\mathrm{d}S$$
$$+\frac{\mathrm{i}\omega}{2g}\int_{C_a}\left(\varphi^{(1)}\varphi_D^{(2)}\frac{\partial\chi}{\partial\rho} + \chi\varphi^{(1)}\frac{\partial\varphi_I^{(2)}}{\partial\rho}\right)\mathrm{d}C \quad (6.15)$$

with $\tilde{Q}_{2D}^{(3)}$ which is now free of double z derivatives:

$$\tilde{Q}_{2D}^{(3)} = \frac{\mathrm{i}\omega}{g}[(2\nabla_0\varphi^{(1)}\nabla_0\varphi_D^{(2)} + 3\nabla_0\varphi_D^{(1)}\nabla_0\varphi_I^{(2)}) + (21\nu^2 - 3k_0^2)\varphi_D^{(1)}\varphi_I^{(2)}$$
$$+(21\nu^2 - \tfrac{1}{2}k_0^2)\varphi^{(1)}\varphi_D^{(2)} + 5\nu(\varphi^{(1)}Q_D^{(2)} + \varphi_D^{(1)}Q_I^{(2)})]. \quad (6.16)$$

By setting first $\chi = H_1(\mu_0\rho)\cos\theta$ and then $\chi = K_1(\mu_n\rho)\cos\theta$, we obtain

$$\int_{-H}^{0}\varphi_{DD1}^{(3)}\mathrm{d}z = -\frac{18\nu C_0^{(3)}}{\mu_0^3 aH_1'(\mu_0 a)}\int_a^\infty H_1(\mu_0\rho)\left[Q_{11}^{(3)} - Q_{1I1}^{(3)} + \tilde{Q}_{2D1}^{(3)} - \mu_0^2\frac{\mathrm{i}\omega}{2g}(\varphi^{(1)}\varphi_D^{(2)})_1\right]\rho\mathrm{d}\rho$$
$$+\sum_{n=1}^{\infty}\frac{18\nu C_n^{(3)}}{\mu_n^3 aK_1'(\mu_n a)}\int_a^\infty K_1(\mu_n\rho)\left[Q_{11}^{(3)} - Q_{1I1}^{(3)} + \tilde{Q}_{2D1}^{(3)} + \mu_n^2\frac{\mathrm{i}\omega}{2g}(\varphi^{(1)}\varphi_D^{(2)})_1\right]\rho\mathrm{d}\rho$$
$$-\frac{\mathrm{i}\omega a}{2g}\left[\frac{18\nu C_0^{(3)}}{\mu_0^3 aH_1'(\mu_0 a)}H_1(\mu_0 a) - \sum_{n=1}^{\infty}\frac{18\nu C_n^{(3)}}{\mu_n^3 aK_1'(\mu_n a)}K_1(\mu_n a)\right]\left(\varphi^{(1)}\frac{\partial\varphi_I^{(2)}}{\partial\rho}\right)_1\Big|_{\rho=a}$$
$$-\frac{\mathrm{i}\omega a}{2g}(\varphi^{(1)}\varphi_D^{(2)})_1|_{\rho=a} \quad (6.17)$$

where $()_1$ and $[]_1$ denote the first Fourier modes of the expressions within the brackets.

With equation (6.10) this is the final expression for the evaluation of the $\varphi_{DD}^{(3)}$ contribution to the force $F^{(3)}$. As in the evaluation of the potential φ_{DD} on the free surface, there are two main problems in the application of this expression. The first one is the local contribution associated with modified Bessel functions $K_1(\mu_n a)$ and the same method as used in the calculation of the local contribution to the potential φ_{DD} on the free surface can be used. In fact the coefficient μ_n^2 which is introduced by the transformation (6.15) is annulled by the integral:

$$\int_{-H}^{0} f_n^{(3)}(z)\mathrm{d}z = -\frac{9\nu}{\mu_n^2} \quad (6.18)$$

and we have the same type of logarithmic singularity.

The second problem concerns the oscillatory integral associated with the Hankel function $H_1(\mu_0 r)$. Since there is no analytical expression for $\varphi_{DD}^{(2)}$ we cannot calculate

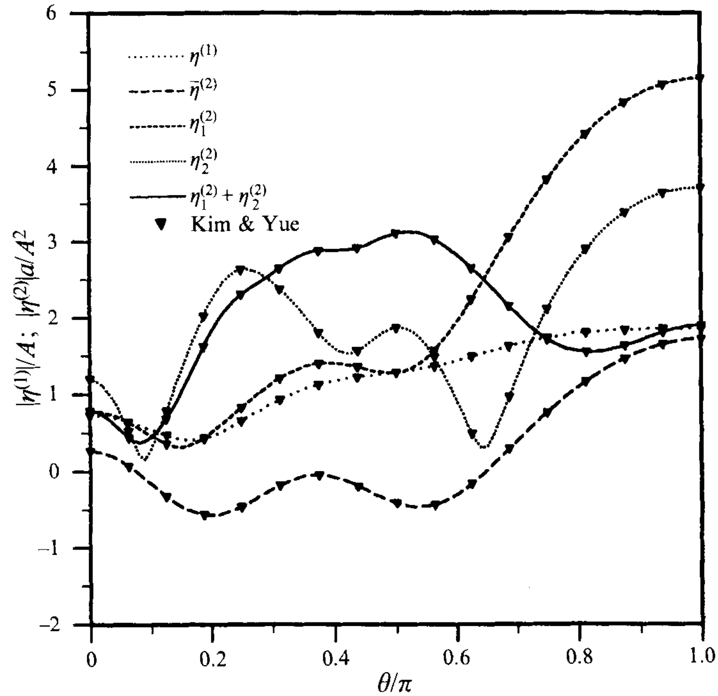

FIGURE 1. First- and second-order components of the free-surface elevation at the waterline, for $H = a, \nu a = 2.0$. Comparison with Kim & Yue's results.

this integral in a semi-analytical way, as in the second-order case, and we must integrate it numerically until convergence. Advantage is taken of the fact that the integral asymptotically oscillates in r at known spatial frequencies (see Appendix A) to filter them out. It was found that convergence is usually reached within two or three wavelengths from the cylinder. We refer to Malenica (1994) for details.

7. Results

The method of calculation was first validated at second order by comparing our results with those obtained by Kim & Yue (1989). Figure 1 shows the free surface elevation at the waterline, compared to Kim & Yue's numerical results. The case considered is $H = a$, $\nu a = 2.0$. The notation is

$$\eta^{(1)} = \frac{\mathrm{i}\omega}{g}\varphi^{(1)}, \tag{7.1}$$

$$\eta_1^{(2)} = -\frac{1}{4g}\nabla\varphi^{(1)}\cdot\nabla\varphi^{(1)} - \frac{\nu^2}{2g}\varphi^{(1)}\varphi^{(1)}, \tag{7.2}$$

$$\eta_2^{(2)} = \frac{2\mathrm{i}\omega}{g}\varphi^{(2)}, \tag{7.3}$$

$$\bar{\eta}^{(2)} = -\frac{1}{4g}\nabla\varphi^{(1)}\cdot\nabla\varphi^{(1)*} + \frac{\nu^2}{2g}\varphi^{(1)}\varphi^{(1)*}, \tag{7.4}$$

these quantities being calculated for $z = 0$. In (7.4) * stands for the complex conjugate. The agreement is excellent.

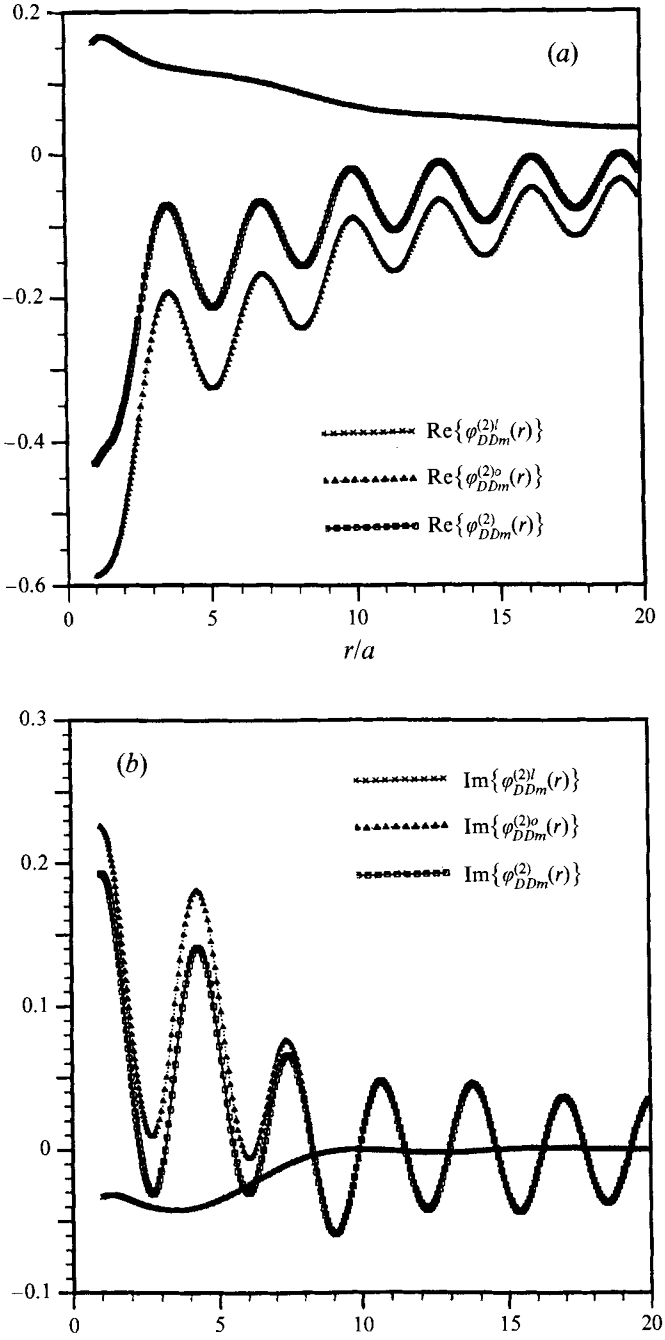

FIGURE 2. First Fourier mode of the second-order diffraction potential $\varphi^{(2)}_{DD}$ at the free surface, with its local and oscillatory components. $H = 10a$; $\nu a = 0.5$. (a) Real parts, (b) imaginary parts.

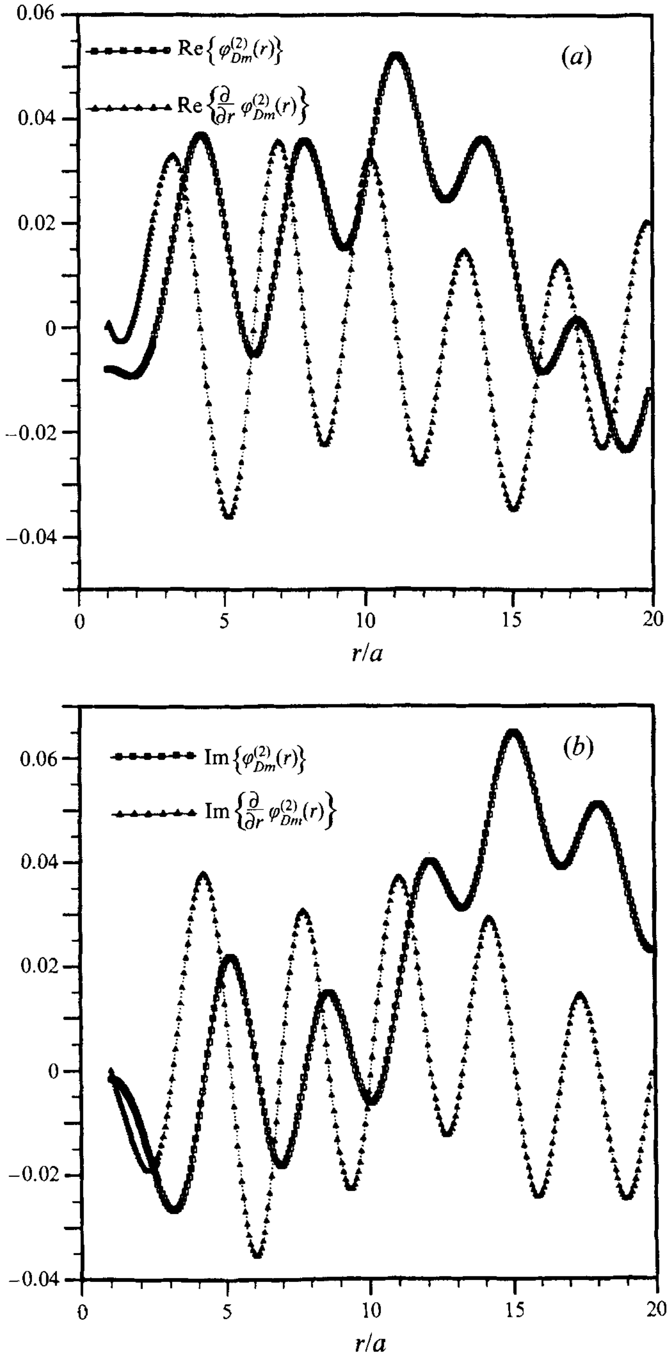

FIGURE 3. Fifth Fourier mode of the total second-order diffraction potential at the free surface, together with its radial derivative. $H = 10a$; $\nu a = 0.5$. (a) Real parts, (b) imaginary parts.

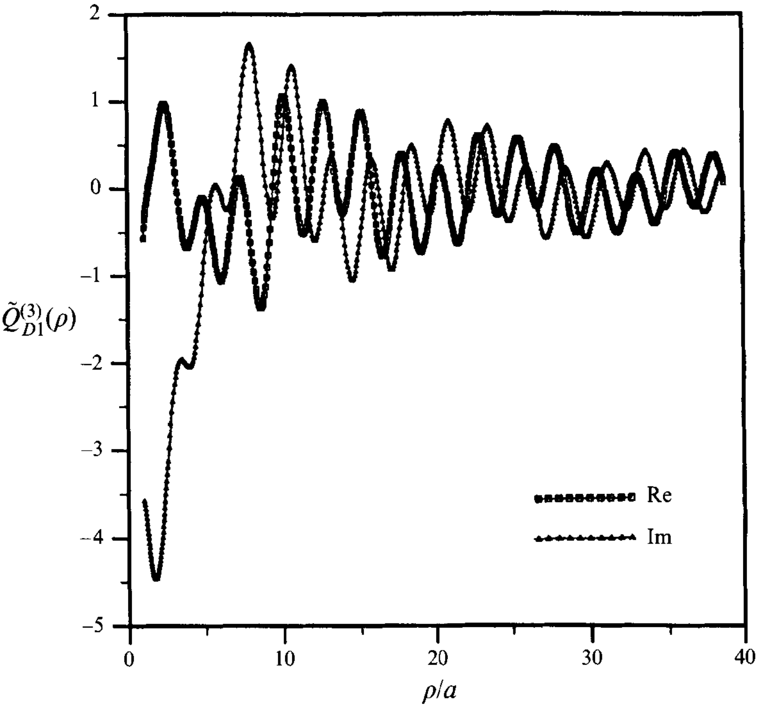

FIGURE 4. Real and imaginary parts of $\tilde{Q}^{(3)}_{D1}$ at the free surface (see equations (7.8) and (6.17)). $H = 10a$; $\nu a = 0.5$.

The figures that follow show intermediate calculation results for the case of a water depth equal to 10 times the cylinder radius ($H/a = 10$), and for $\nu a = 0.5$.

Figure 2 shows the local and oscillatory contributions to the second-order diffraction potential $\varphi^{(2)}_{DDm}(r,z)$ for $m = 1$ and $z = 0$ (at the free surface). The three curves correspond to the real and imaginary parts of

$$\varphi^{(2)o}_{DDm}(r,0) = \pi \mathrm{i} C^{(2)}_0 H_m(\kappa_0 r) \int_a^r [J_m(\kappa_0\rho) - Z^{(2)}_{m0} H_m(\kappa_0\rho)] Q^{(2)}_{Dm}(\rho)\rho \mathrm{d}\rho$$
$$+ \pi \mathrm{i} C^{(2)}_0 [J_m(\kappa_0 r) - Z^{(2)}_{m0} H_m(\kappa_0 r)] \int_r^\infty H_m(\kappa_0\rho) Q^{(2)}_{Dm}(\rho)\rho \mathrm{d}\rho, \qquad (7.5)$$

$$\varphi^{(2)l}_{DDm}(r,0) = 2\sum_{n=1}^{\infty} C^{(2)}_n K_m(\kappa_n r) \int_a^r [I_m(\kappa_n\rho) - Z^{(2)}_{mn} K_m(\kappa_n\rho)] Q^{(2)}_{Dm}(\rho)\rho \mathrm{d}\rho$$
$$+ 2\sum_{n=1}^{\infty} C^{(2)}_n [I_m(\kappa_n r) - Z^{(2)}_{mn} K_m(\kappa_n r)] \int_r^\infty K_m(\kappa_n\rho) Q^{(2)}_{Dm}(\rho)\rho \mathrm{d}\rho, \qquad (7.6)$$

$$\varphi^{(2)}_{DDm}(r,0) = \varphi^{(2)o}_{DDm}(r,0) + \varphi^{(2)l}_{DDm}(r,0). \qquad (7.7)$$

Then figure 3 shows the real and imaginary parts of the total second-order diffraction potential $\varphi^{(2)}_{Dm}(r,z)$ for $m = 5$ and $z = 0$, together with its first radial derivative (obtained numerically by finite differenciation).

We now come to the calculation of the free surface integral (6.17), where the

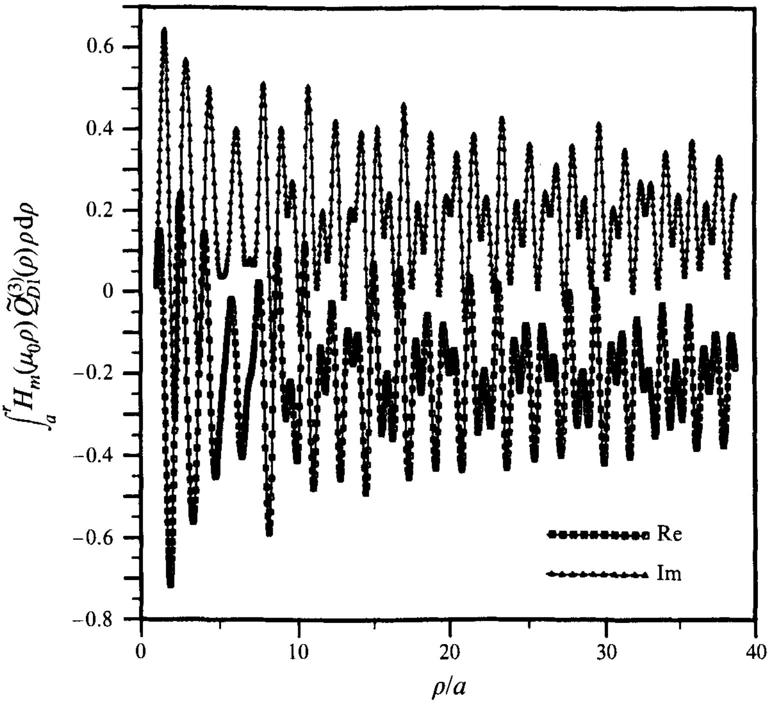

FIGURE 5. Free surface integral (see equation (7.9)). $H = 10a$; $\nu a = 0.5$.

difficulty resides with the first term, because of its oscillatory nature. Figure 4 shows the real and imaginary parts of $\tilde{Q}_{D1}^{(3)}$, defined as

$$\tilde{Q}_{D1}^{(3)} = Q_{11}^{(3)} - Q_{1I1}^{(3)} + \tilde{Q}_{2D1}^{(3)} - \mu_0^2 \frac{\mathrm{i}\omega}{2g} (\varphi^{(1)} \varphi_D^{(2)})_1, \tag{7.8}$$

and figure 5 shows the oscillatory integral $I(r)$, defined as

$$I(r) = \int_a^r H_1(\mu_0 \rho) \tilde{Q}_{D1}^{(3)}(\rho) \rho \mathrm{d}\rho. \tag{7.9}$$

From this figure it does not look as if convergence is going to be quickly attained when r increases. The same kind of problem occurs at second order, and the same remedy as used in Molin & Marion (1986) has been utilized here: advantage is taken of the fact that the leading-order oscillations of $I(r)$ are known (see Appendix A) to filter them out numerically. When $\nu H > 3$ (deep water) it is particularly easy because the oscillatory pattern repeats itself at half-wavelength intervals (we then have $\kappa_0 = 4k_0$ and $\mu_0 = 9k_0$).

Finally we present results for the third-order horizontal load $F^{(3)}$ which is decomposed into three components:

$F_1^{(3)}$ is the part which comes from triple products of first-order quantities:

$$F_1^{(3)} = -\frac{\mathrm{i}\omega}{8g} \varrho \int_{C_{B0}} [\varphi^{(1)} (\nabla \varphi^{(1)})^2 + \nu^2 (\varphi^{(1)})^3] \boldsymbol{n} \mathrm{d}C; \tag{7.10}$$

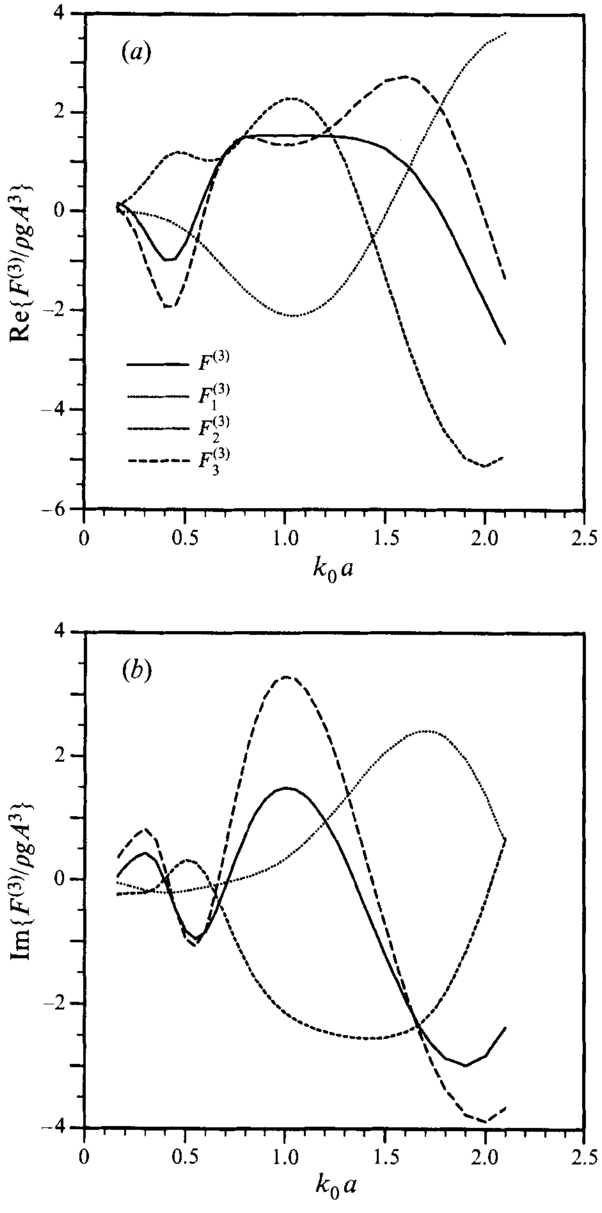

FIGURE 6. Third-order horizontal force on a vertical cylinder, decomposed in its three components. $H = 10a$. (*a*) Real parts, (*b*) imaginary parts.

$F_2^{(3)}$ from products of first-order and second-order quantities:

$$F_2^{(3)} = -\frac{1}{2}\varrho \iint_{S_{B0}} \nabla\varphi^{(1)} \cdot \nabla\varphi^{(2)} \boldsymbol{n} \mathrm{d}S - \varrho\nu \int_{C_{B0}} \varphi^{(1)}\varphi^{(2)} \boldsymbol{n} \mathrm{d}C; \tag{7.11}$$

and $F_3^{(3)}$ due to the third-order potential:

$$F_3^{(3)} = 3\mathrm{i}\omega\varrho \int_{S_{B0}} \varphi^{(3)} \boldsymbol{n} \mathrm{d}S. \tag{7.12}$$

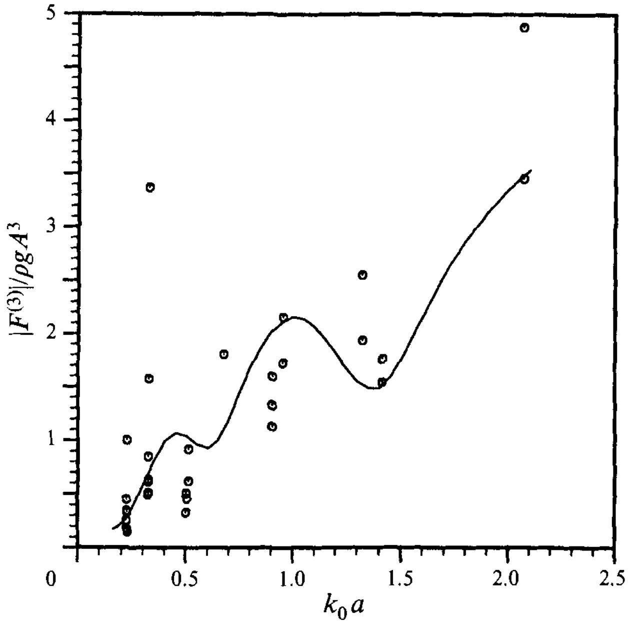

FIGURE 7. Modulus of the third-order horizontal force, compared to experimental results. $H = 10a$ for the calculations.

Still for $H/a = 10$, figure 6 shows the real and imaginary parts of these three components (as functions of $k_0 a$), together with their sum. It can be seen that all contributions are important. Figure 7 shows the modulus of $F^{(3)}$, together with experimental results. These results were obtained by re-analysing data from experiments carried out within the scope of the VRMTLP Project (Moe 1993). The tested cylinder is a 1:40 scale model of one column of the Snorre TLP (radius: 12.5 m; draught: 37.5 m). These tests were considered as more reliable than others because they had produced second-order loads in very good agreement with calculated values. Unfortunately, as can be seen from the figure, the third-harmonic component of the measured force shows quite an appreciable scatter and no definitive conclusion can be drawn from the comparison. The objection can be made that the Snorre TLP column has little in common with a cylinder going all the way down to the sea floor. For $k_0 a > 1$ the first-order wave field hardly reaches the bottom of the column and both structures can be regarded as equivalent (for the first- and third-order loads; not for the second-order ones!). As a matter of fact, when comparing figure 6(a) with figure 8(a), which relates to the case $k_0 H = 8$, little differences can be seen at low $k_0 a$ values. This shows that, unlike second-order ones, third-order pressures are localized near the free surface.

Since ringing occurs in long waves, with typical $k_0 a$ values in the range 0.15—0.25, we present in figure 8 the real and imaginary parts of the third-order force, for $0 < k_0 a < 0.25$. In these calculations the water depth H varies with $k_0 a$ so that $k_0 H$ remains equal to 8. Calculations were also performed at $k_0 H = 4$ and gave identical results, showing again that third-order pressures do not penetrate the water column deeply.

As mentioned in the Introduction, some authors have suggested that long-wave theories could be used to predict the nonlinear components of the loading at low

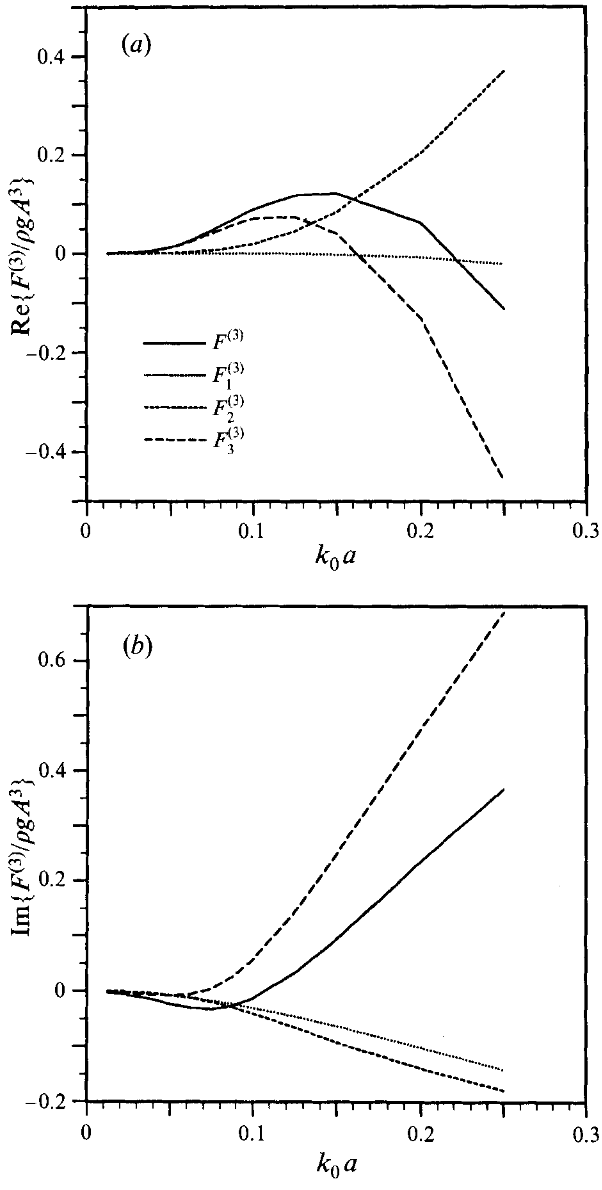

FIGURE 8. Third-order force for $k_0a < 0.25$ and $k_0H = 8$. (*a*) Real parts, (*b*) imaginary parts.

k_0a values. Faltinsen *et al.* (1995) give the third-order horizontal force, for k_0a and $k_0A \to 0$, as asymptotically equal to

$$F^{(3)} = -2\,\mathrm{i}\,\pi\,\varrho\,g\,k_0^2a^2\,A^3 \tag{7.13}$$

with $F_1^{(3)}$ accounting for one half, and $F_2^{(3)}$ and $F_3^{(3)}$ for one fourth each. These asymptotic values are plotted on figure 9, which is a blow-up of figure 8(*b*) for $0 < k_0a < 0.05$. For $F_1^{(3)}$ and its asymptotic value, we observe a good agreement, which actually extends to k_0a values over 0.10. However $F_2^{(3)}$ and $F_3^{(3)}$ depart from the theoretical values given by Faltinsen *et al.* much earlier, for k_0a around 0.02. Further comparisons between our results and Faltinsen *et al.*'s are given in Appendix B.

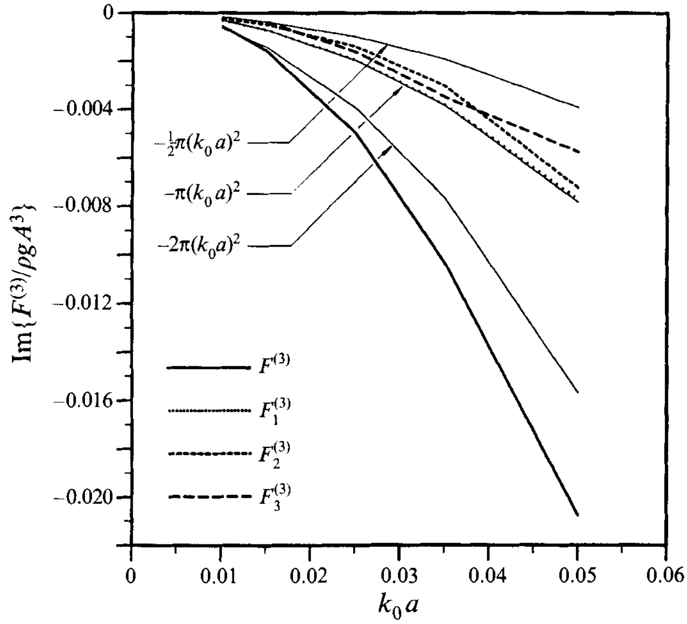

FIGURE 9. Imaginary part of the third-order force, for $k_0 a < 0.05$ and $k_0 H = 8$, compared with the asymptotic results of Faltinsen *et al.*

8. Discussion

An important result obtained in this analysis is that long-wave theories may not be applicable to the calculation of triple-frequency loads. As a matter of fact we did not expect them to do well for $k_0 a > 0.05$, the reason being that their domain of validity seems to shrink as the square of the order of the load that they are used to predict: at first-order, the Morison equation with $1 + C_m = 2$ does predict accurately the diffraction loads for $k_0 a < 0.50$. At second-order the agreement with the exact calculations (accounting for the second-order diffraction potential) is limited to $k_0 a < 0.12$. Since the double-frequency free waves are four times shorter (in deep water) than the first-order ones, it is tempting to infer that the significant parameter is $k_0 a$ at first order, $\kappa_0 a$ at second order, and $\mu_0 a$ at third order. $\mu_0 a$ less than 0.50 means $k_0 a$ less than 0.05.

From the results shown on figure 9, it looks as if 0.05 was too optimistic a figure and that it must be cut by half.

Another conclusion that can be drawn from these considerations is that the spatial resolution of the problem must be in accordance with the free wavelength at frequency 3ω $(2\pi/\mu_0)$. This is no problem with the numerical method employed here, owing to the Fourier series decomposition in the polar angle which reduces integrations on the free surface to line integrals. But it could be a problem in three-dimensional numerical wave tanks, since it means that the first-order wavelength needs to be discretized into about 100 elements. The resulting number of panels might be prohibitive.

Our final comment is on validation. We have checked our developments and calculations as thoroughly as possible, but it is quite regretable that there be no reliable experimental data to confirm them. The same problem has plagued the development of second-order diffraction theory for years. Improvements in the experimental techniques have become a major issue for the progress of hydrodynamics.

This work was carried out within the scope of the CLAROM project: 'high frequency resonances of offshore structures', partly supported by the French Ministry of Industry. Partners in this project are Bureau Veritas, Doris Engineering, IFP, Ifremer, Principia and Sirehna.

Appendix A. Far-field behaviour of the third-order diffraction potential

Here we want to show that integrals such as

$$I_\infty = \lim_{\rho\to\infty} \int_{S_\infty} \left[G(\boldsymbol{x},\xi)\frac{\partial\varphi_{DD}(\xi)}{\partial\rho} - \varphi_{DD}(\xi)\frac{\partial G(\boldsymbol{x},\xi)}{\partial\rho} \right] \mathrm{d}S \tag{A 1}$$

which are involved in the integral equation (3.18) are zero.

The radiation condition for the second-order diffraction potential has long been a controversial issue. In Molin's original analysis (1979), it was tentatively shown that, at large radial distances, the second-order diffraction potential, to the leading order ($O(A^2/\rho^{1/2})$), consists of two components: waves 'locked' to the first-order wave-field, with local wavenumber vector $\boldsymbol{k}_{0I} + \boldsymbol{k}_{0\theta}$ ($\boldsymbol{k}_{0I}$ being the wavenumber vector of the incoming waves, and $\boldsymbol{k}_{0\theta}$ the local wavenumber vector of the first-order diffracted waves, in the radial direction); and 'free' waves, travelling in the radial direction with wavenumber κ_0 (given by $4\omega^2 = g\kappa_0 \tanh\kappa_0 H$). Even though this result was not established on purely rigorous mathematical grounds, it has now been accepted as being correct.

This result comes out straightforwardly when one assumes that, far away from the body, the first-order diffraction waves can locally be regarded as plane waves traveling in the radial direction. The second-order analysis of such a dual plane wave system is easy and gives the locked waves. Radial free waves then must be added to account for the nonlinearities occurring in the vicinity of and on the structure.

Here we just assume that the same kind of approach can be used to determine the far-field wave system of the third-order diffraction potential. The result is that, to the leading order $O(A^3/\rho^{1/2})$, the third-order diffraction potential consists of three components: 'locked' waves with wavenumber vector $2\boldsymbol{k}_{0I} + \boldsymbol{k}_{0\theta}$; 'locked' waves with wavenumber vector $\boldsymbol{k}_{0I} + \boldsymbol{\kappa}_{0\theta}$; and 'free' waves, travelling in the radial direction, with wavenumber μ_0 given by $9\omega^2 = g\mu_0 \tanh\mu_0 H$.

To summarize, the diffraction potential admits, at first, second, and third order, the following far-field expressions:

first-order

$$\varphi_D^{(1)} \sim \frac{f_D(\vartheta)}{\rho^{1/2}} f_0^{(1)}(\zeta)\mathrm{e}^{\mathrm{i}k_0\rho} + O(\rho^{-3/2}), \tag{A 2}$$

second-order

$$\varphi_D^{(2)}(\rho,\vartheta) \sim \frac{h_{DL}(\vartheta)}{\rho^{1/2}}\frac{\cosh K_1(\zeta+H)}{\cosh K_1 H}\mathrm{e}^{\mathrm{i}k_0\rho(1+\cos\vartheta)} + \frac{h_{DF}(\vartheta)}{\rho^{1/2}}\frac{\cosh\kappa_0(\zeta+H)}{\cosh\kappa_0 H}\mathrm{e}^{\mathrm{i}\kappa_0\rho} + O(\rho^{-1}), \tag{A 3}$$

third-order

$$\varphi_D^{(3)}(\rho,\vartheta) \sim \frac{q_{1DL}(\vartheta)}{\rho^{1/2}}\frac{\cosh K_2(\zeta+H)}{\cosh K_2 H}\mathrm{e}^{\mathrm{i}k_0\rho(1+2\cos\vartheta)} + \frac{q_{2DL}(\vartheta)}{\rho^{1/2}}\frac{\cosh K_3(\zeta+H)}{\cosh K_3 H}\mathrm{e}^{\mathrm{i}\rho(\kappa_0+k_0\cos\vartheta)} + \frac{q_{DF}(\vartheta)}{\rho^{1/2}}\frac{\cosh\mu_0(\zeta+H)}{\cosh\mu_0 H}\mathrm{e}^{\mathrm{i}\mu_0\rho} + O(\rho^{-1}), \tag{A 4}$$

where

$$K_1 = k_0(2(1+\cos\vartheta))^{1/2}, \quad K_2 = k_0(5+4\cos\vartheta)^{1/2}, \quad K_3 = (k_0^2+\kappa_0^2+2k_0\kappa_0\cos\vartheta)^{1/2} \tag{A 5}$$

are the wavenumbers of the locked waves, K_1 at second order, and K_2, K_3 at third order.

Knowing the far-field behaviour of the Green function and using the stationary phase method we can easily deduce the asymptotic behaviour of the integrals I_∞:

$$I_\infty^{(2)} \sim \frac{1}{\rho^{1/2}}[h_1 e^{i\rho(\kappa_0+4k_0)} + h_2 e^{i\rho\kappa_0}], \tag{A 6}$$

$$I_\infty^{(3)} \sim \frac{1}{\rho^{1/2}}[q_1 e^{i\rho(\mu_0+3k_0)} + q_2 e^{i\rho(\mu_0+\kappa_0+k_0)} + q_3 e^{i\rho(\mu_0-k_0)} + q_4 e^{i\rho(\mu_0+\kappa_0-k_0)}], \tag{A 7}$$

which are thus zero when $\rho \to \infty$.

Appendix B. Comparison with Faltinsen *et al.*'s (1995) theory

As mentioned in the Introduction, Faltinsen *et al.*'s theory rests upon different assumptions, namely both the cylinder radius a and the wave amplitude A are assumed to be small, and of the same order. In our approach only A is small (compared with the wavelength). So it is not obvious that both sets of results are comparable. Still we believe they must be, because Faltinsen *et al.* produced a triple-frequency load that is $O(A^3)$, that is third order in the wave amplitude, just like ours. So their and our triple frequency loads should agree in the limit $ka \to 0$.

In this Appendix we report two further comparisons between Faltinsen *et al.*'s theory and ours, dealing with the second-order (double harmonic) potential, and the $F_2^{(3)}$ component to the third-order loads.

The second-order diffraction potential is given by Faltinsen *et al.* as

$$\varphi_D^{(2)} = -i\omega\, k_0\, A^2\, a\ (\psi_0(r,z) + \psi_2(r,z)\ \cos 2\theta) \tag{B 1}$$

(their equation (3.14), with a correction in sign to account for our slightly different conventions).

From Faltinsen *et al.*'s figure 3, at the waterline ($r = a$, $z = 0$), ψ_2 is equal to 0.8. So we present on figure 10, as functions of $k_0 a$, our calculated values of the imaginary parts of $\varphi_{D2}^{(2)}(a,0)/A^2$, together with the curve $-0.4\,\omega\, k_0$ (a being equal to 1 m, and $k_0 H$ to 8. ψ_2 has been divided by 2 according to our convention – see (3.8)). As in figure 2(a), we have separated the local and the oscillatory component $\varphi_{D2}^{(2)}$. We can see that our local component and Faltinsen *et al.*'s simple result do merge together when $k_0 a \to 0$, while the oscillatory component goes to zero at a much faster rate. However it is not negligible for $k_0 a > 0.05$.

The second comparison that we show deals with the $F_2^{(3)}$ component to the third-order load. It is simply given by Faltinsen *et al.* as

$$F_2^{(3)} = -\tfrac{1}{2} i\, \pi\, \rho\, g\, k_0^2\, a^2\, A^3 \tag{B 2}$$

while in our approach it consists of two terms:

$$F_2^{(3)S} = -\frac{1}{2}\rho \iint_{S_{B0}} \nabla\varphi^{(1)} \cdot \nabla\varphi^{(2)}\, \boldsymbol{n}\, dS \tag{B 3}$$

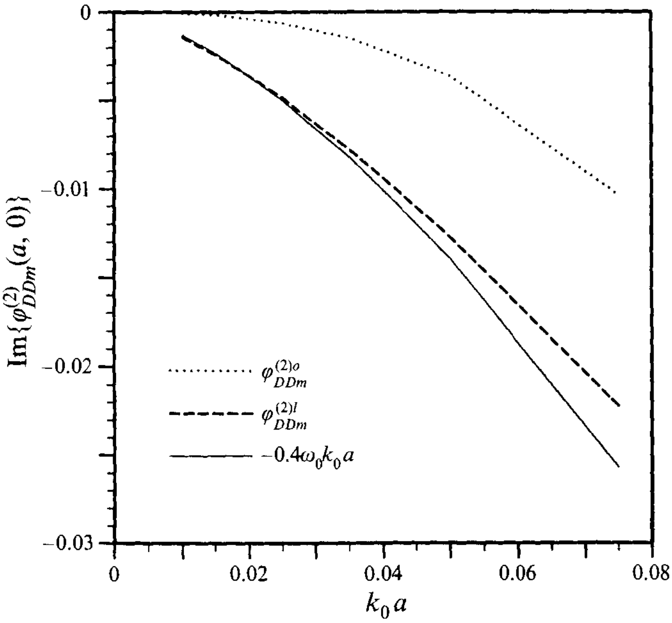

FIGURE 10. Imaginary part of the second-order diffraction potential $\varphi^{(2)}_{DD2}$ at the waterline, compared to the theoretical result of Faltinsen *et al.*

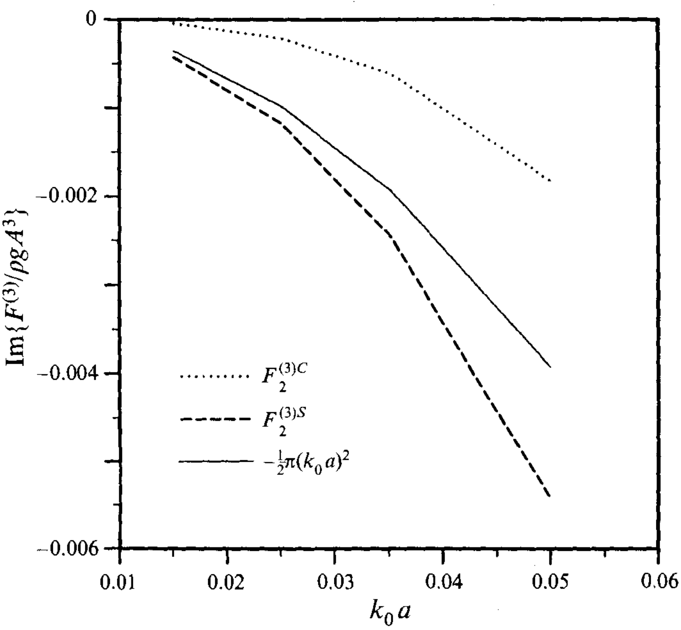

FIGURE 11. $F^{(3)}_2$ component to the third-order force, compared to the theoretical result of Faltinsen *et al.*

and

$$F_2^{(3)C} = -\rho\, v \int_{C_{B0}} \varphi^{(1)}\, \varphi^{(2)}\, \boldsymbol{n}\, \mathrm{d}C. \tag{B 4}$$

According to Faltinsen *et al.*'s theory the first term is dominant, the second one being of a higher order in $k_0 a$.

Figure 11 shows those three components, plotted versus $k_0 a$. Again, the values given by equations (B2) and (B3) do merge together when $k_0 a \rightarrow 0$, while those given by equation (B4) do appear to be of higher order. However when one adds up $F_2^{(3)S}$ and $F_2^{(3)C}$, deviations from the asymptotic result very quickly occur when $k_0 a$ increases from zero. The difference is already about 50 % for $k_0 a = 0.035$.

REFERENCES

CHAU, F. P. & EATOCK TAYLOR, R. 1992 Second-order wave diffraction by a vertical cylinder. *J. Fluid Mech.* **240**, 571–599.

CHEN, X-B., MOLIN, B. & PETITJEAN, F., 1991 Faster evaluation of resonant exciting loads on tension leg platforms. *Proc. VIII Intl Symp. Offshore Engng, Brasil Offshore '91, Rio de Janeiro.*

COINTE, R. 1990 Numerical simulation of a wave channel. In *Engineering Analysis with Boundary Elements*, **7**, 167–177.

EATOCK TAYLOR, R. & CHAU, F. P. 1992 Wave diffraction theory. Some developments in linear and nonlinear theory. *J. Offshore Mech. Arctic Enging* **114**, 185–194.

EATOCK TAYLOR, R. & HUNG, S. M. 1987 Second-order diffraction forces on a vertical cylinder in regular waves. *Appl. Ocean Res.* **9**, 19–30.

FALTINSEN, O. M., NEWMAN, J. N. & VINJE, T. 1995 Nonlinear wave loads on a slender vertical cylinder. *J. Fluid Mech.* **289**, 179–198.

FENTON, J. D. 1978 Wave forces on vertical bodies of revolution. *J. Fluid Mech.* **85**, 241–255.

FERRANT, P. 1994 Radiation and diffraction of nonlinear waves in three dimensions. *Proc. 7th Intl Conf. on the Behaviour of Offshore Structures, BOSS'94, Cambridge, USA.*

JEFFERYS, E. R. & RAINEY, R. T. C. 1994 Slender body models of TLP and GBS ringing. *Proc. 7th Intl Conf. on the Behaviour of Offshore Structures, BOSS'94, Cambridge, USA.*

KIM, M. H. & YUE, D. K. P. 1989 The complete second-order diffraction solution for an axisymmetric body. Part 1. Monochromatic incident waves. *J. Fluid Mech.* **200**, 235–264.

LIGHTHILL, M. J. 1979 Waves and hydrodynamic loading. *Proc. 2nd Intl Conf. on the Behaviour of Offshore Structures, BOSS'79, London.*

MADSEN, O. S. 1986 Hydrodynamic force on circular cylinders. *Appl. Ocean Res.* **8**, 151–155.

MALENICA, Š. 1994 Diffraction de troisième ordre et interaction houle-courant pour un cylindre vertical en profondeur finie. PhD dissertation, Paris 6 University (in French).

MEI, C. C. 1983 *The Applied Dynamics of Ocean Surface Waves.* Wiley Interscience.

MOE, G. (Ed.) 1993 Vertical Resonant Motions of TLP's. Final Report. *NTH Rep.* R-1-93.

MOLIN, B. 1979 Second-order diffraction loads upon three dimensional bodies. *Appl. Ocean Res.* **1**, 197–202.

MOLIN, B. & MARION, A. 1986 Second-order loads and motions for floating bodies in regular waves. *Proc. 5th Intl Symp. Offshore Mechanics and Arctic Engng, Tokyo.*

NEWMAN, J. N. & LEE, C-H. 1992 Sensitivity of wave loads to the discretization of bodies. *Proc. 6th Intl Conf. on the Behaviour of Offshore Structures, BOSS'92, London.*

RAINEY, R. C. T. 1989 A new equation for wave loads on offshore structures. *J. Fluid Mech.* **204** 295–324.

ROMATE, J. E. 1989 The numerical simulation of nonlinear gravity waves in three dimensions using a higher order panel method. PhD dissertation, University of Twente, The Netherlands.

SCOLAN, Y-M. & MOLIN, B. 1989 Second-order deformation of the free surface around a vertical cylinder. Part 2. *Proc. 4th Intl Workshop Water Waves and Floating Bodies, Oystese.*